ACTIVE CABIN VIBRATION REDUCTION FOR JET-SMOOTH HELICOPTER RIDE

Falk Hoffmann, Peter Konstanzer, Martijn Priems,
EUROCOPTER Deutschland GmbH, Munich, Germany

Jerome Chemin, EUROCOPTER SAS, Marignane, France

Abstract

A new innovative approach for active control of rotor induced vibrations within the cabin for light and medium H/C is presented. Compared to current passive or semi-active mass-spring systems, which produce nodal points at the actuator clamping position, vibration control with variable local accentuation is possible, depending on the location of sensors used for control. This paper presents an overview of the system design and describes the most important results achieved during several flight tests on different light and medium rotorcrafts.

NOMENCLATURE

AF	Anti Aliasing Filter
A/D	Analogue Digital Converter
AVC	Active Vibration Control
C	C(jω) - Matrix of Transfer Functions between Error and Control Signals
CH	Hermitian Matrix of C
D/A	Digital Analogue Converter
DSP	Digital Signal Processor
FG	Force Generator
FIR	Finite Impulse Response
FxLMS	Filtered-x-LMS
H/C	Helicopter
LMS	Least Mean Square
M	Number of Sensors
MIMO	Multiple Input Multiple Output
N	Number of Actuators
NF	Number of Controlled Harmonics
RF	Reconstruction Filter
SYS-ID	System Identification
T	Sampling Period
α	Step Size
β	Leakage
$\underline{e}$	$\underline{e}(j\omega)$ Vector of Error Signals at Control Frequency
$\underline{p}$	$\underline{p}(j\omega)$ Vector of Primary Disturbance
$\underline{y}$	$y(j\omega)$ Vector of Actuator Driving Signal
$y(nT)$	Vector of Control Signals at Discrete Time
ω_0	Control Frequency

1. INTRODUCTION

The helicopter main rotor operates in a complex highly asymmetric turbulent aerodynamic environment, which creates oscillations in the flexible rotor blades. The resulting forces and moments, transmitted through the rotor hub, cause rotor induced vibrations. This is the main source of vibrations in modern helicopters, with impact on safety, health and comfort for crew as well as passengers.

Many passive approaches for vibration isolation have been developed and successfully implemented during the last decades. Passive anti-resonance isolation systems like ARIS or SARIB as well as classical vibration absorbers and pendulum absorbers are just some examples of presently flying systems, which were suitable to meet the current customer needs [1].

Future rotorcrafts, however, have to be designed to answer new tightened demands and limits described by, for instance, the European parliament in DIRECTIVE 2002/44/EC on vibration. In addition, the global aim on reducing the environmental impact of rotary air transport, forces helicopter manufactures to provide effective solutions. The

tendency is to vary the rotor speed over an extended range in order to optimize for both low external noise levels and high fuel efficiency. This implicitly results in substitution of commonly used passive tuned systems, with their limited efficiency and emphasizes the need of active and adaptive vibration reduction.

A new innovative multi-axis and multi-frequency AVC system for jet-smooth helicopter ride has been developed and flight tested on several light and medium rotorcrafts. The system was designed to fit the low cost, compact and light weight requirements and was optimized as an upgrade to current technology which makes it retrofittable to the present fleet.

2. AVC SYSTEM DESCRIPTION

Active vibration control systems use the phenomenon of destructive interference between the primary disturbance and the inverse secondary signal produced by a control unit. The superposition of this artificial vibration field with the natural rotor-induced vibration field leads to global vibration minimization with variable local accentuation. In principle, such a system consists of a set of actuators, transducers for vibration sensing, voltage amplifiers and an adequate control unit. A schematic block diagram of the control loop, which has been used for helicopter cabin vibration reduction, shows Fig. 1.

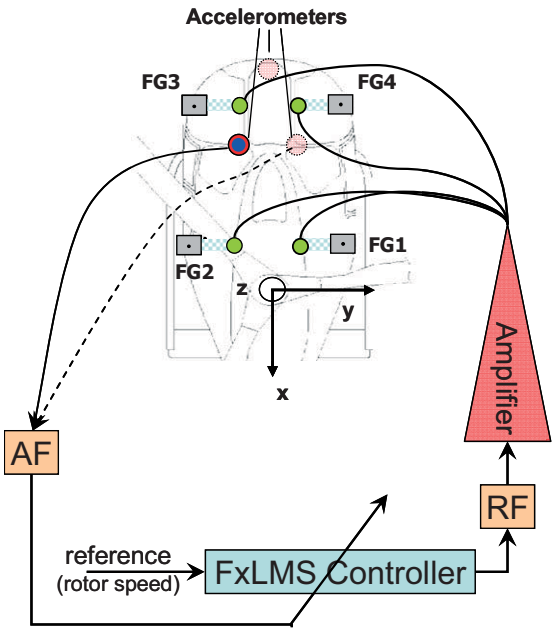

Figure 1: Schematic block diagram of the AVC system.

All actuators (FG1-FG4) are driven by one control unit to minimize vibrations at an arbitrary position of interest, e.g. at the pilot seat, passenger seat as well as in the rear compartment. Standard Triaxial ICP® accelerometers from PCB Piezotronics were installed directly on the cabin floor. These accelerometers were used as error sensors in the control loop. The hardware also comprises analogue low-pass filters (Butterworth) to avoid aliasing and unwanted high frequency excitation of actuator prototypes. The FxLMS algorithm was implemented on an 'off the shelf' DSP system in the programming language C.

2.1. Prototype Actuator Concept

For the narrowband application the force generator is designed in a near-resonance condition, i.e. the frequency range of operation is in the vicinity of the force generator eigenfrequency. This yields to a dynamic amplification of the generated control forces and contributes to the specific high force requirement.

The actuator is designed to fit the standard attachment of current passive absorbers and to ensure simple substitution (retrofittable) without significant structural modification of the helicopter.

The prototype force generator is optimized for high forces, high endurance and low frequencies. It is based on a leaf-spring cantilever beam design and consists of five layers: three glass fibre GFRP layers (top, middle, down) and two active layers of solid state material. The operating principle is the following: to induce bending into the leaf-spring the active layers are driven in an antagonistic way, i.e. the upper layer extends whereas the bottom layer retracts [2].

Based on this active leaf-spring design, the force generator provides direct electrical control of forces by the inertia of its attached mass and combines the challenging requirements like high bandwidth with very compact design. A schematic representation of the prototype actuator and a picture of the realized module are given in following figure.

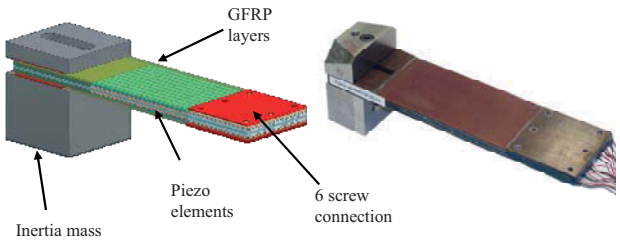

Figure 2: Prototype actuator (inertial force generator)

2.2. Control Approach

Rotor induced vibrations show in principle tonal character with significant variations in amplitude and

phase depending on flight conditions. Since these frequencies are changing with rotor speed, the control concept has to deal with these variations in amplitude and phase. For this reason the control approach chosen here is the narrowband MIMO filtered-x version of the adaptive LMS algorithm.

The controller works in principle like an adaptive band pass filter (FIR) with high gain at the centre frequency. In order to obtain the optimum filter coefficients, the gradient of the error performance surface has to be zero. Thus, gradient based adaptation algorithms are used to update the tap weights of the filter. Since the LMS algorithm just needs an estimation of the gradient of the error surface instead the gradient itself, the approach becomes very simple and capable for many applications. The basic LMS algorithm could be implemented if there were no secondary path dynamics in the system. However, in practice, there are dynamics involved in the secondary path produced by the hardware (amplifier, actuators, filters etc.) and by variations in the transfer path properties between actuator and error sensor. For this reason, the filtered-x LMS algorithm was applied, which pre-filters the reference signal with the estimated plant response C_{est} in a way that the measured error signal and filtered reference signal are again aligned in time to give a valid cross-correlation estimate. This secondary transfer function matrix C_{est} comprises the complete dynamic behaviour of the force generator, the anti aliasing filters as well as the time lag due to calculation of the algorithm and D/A and A/D conversion. As a consequence, the FxLMS algorithm is fairly robust until the secondary path is time varying. In this case, online system identification should be used once in a while.

A block diagram of the practical implementation of the time domain filtered-x LMS algorithm with a model C_{est} (gained by SYS-ID) of the true plant response C shows Figure 3.

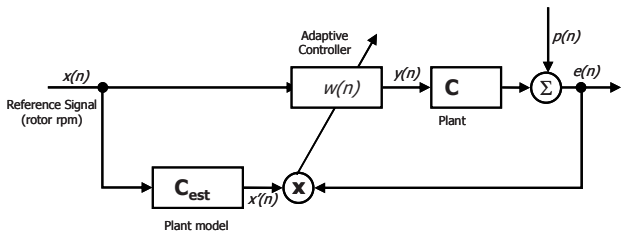

Figure 3: Block diagram of the FxLMS control loop

Inputs of the controller are the reference signal and the error signals *e*. The outputs of the controller are the actuator signals *y*. The control strategy used to adjust the output of actuators is to minimize the sum of the mean square outputs of a number of sensors. The detected sensor signal itself can be described as the superposition of the primary disturbance *p* with the artificial secondary vibration. This dependency of the error signal *e* from the control signal *y* describes the following equation:

$$e(n) = p(n) + Cy(n) \tag{1}$$

The filtered-reference LMS algorithm attempts to minimise the mean-square value of the measured error signal. Another objective would be to minimise the sum of the mean-square error and the weighted squared control filter coefficients, which has certain practical advantages. The cost function to be minimized is then given by:

$$J = E\left\{e^2(n)\right\} + \beta w^T w \tag{2}$$

The leakage parameter β can be considered as a weighting factor for the control effort. If the error signal becomes zero, the coefficients would 'leak' away in this algorithm because of the leakage term*(1-$\alpha\beta$)*. After derivation of equation (2), the rule to adapt the control filter coefficients at every sample point can be written as:

$$\underline{w}(n+1) = (1-\alpha\beta)\underline{w}(n) - \alpha\,\underline{x}'(n)\underline{e}(n) \tag{3}$$

This adaptation rule must be normally computed at every sample time, which can be a considerable computational burden. For this reason the filter update was implemented in the frequency domain so that the time-domain convolution becomes to a multiplication in the frequency domain, even though the control filter is implemented in the time domain. For a constant frequency ω, the FxLMS algorithm represents a time invariant and linear transfer block with a fixed impulse response. To obtain the actuator driving signal *y(nT)* from the controller output $h^n(\omega)$, an inverse transformation must be performed as Eq. (4) shows.

$$y(nT) = \mathrm{Re}\left\{h^n e^{j\omega_0 nT}\right\} \tag{4}$$

Depending on the applied integration rule (in this case forward rectangular) and taking the leakage factor into account, $h^n(\omega)$ becomes to:

$$h^n = h^{n-1}\cdot(1-2\alpha\beta) - 2\alpha C^H \cdot e\left((n-1)T\right)\cdot e^{-j\omega_0(n-1)T} \tag{5}$$

After transforming the complex numbers into trigonometric functions, the impulse response for one controlled frequency is:

$$y(nT) = -\frac{2\alpha K^n}{K}\cdot|C|\cdot\cos(\omega nT - \phi_C) \tag{6}$$

with: $K = (1 - 2\alpha\beta)$ and with $C = |C(j\omega)|e^{j\phi_C}$.

After z-transformation the new transfer functions of the controller becomes to:

$$(7)\ F(z) = -\frac{2\alpha}{K} \cdot |C| \cdot \frac{\cos(\phi_C) z^2 - zk\cos(\omega T + \phi_C)}{z^2 - 2zk\cos(\omega T) + k^2}$$

The narrowband FxLMS algorithm is a control approach that adapts a band pass filter (FIR) to a reference signal, which is the frequency to be controlled. The basic structure of the control loop shows Figure 4.

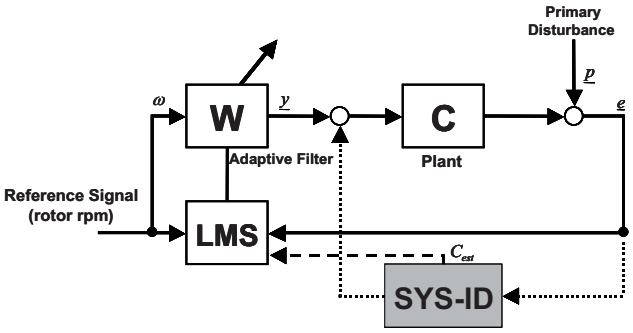

Figure 4: Block diagram of narrowband FxLMS control loop with SYS-ID

As mentioned before, the controller needs an adequate characterization of the dynamics within the plant. This is typically realized by a SYS-ID procedure, producing a set of transfer functions in a frequency range of interest. For this purpose, the actuator is driven with a chirp. Owing to the fact that the transfer functions of the force generator may depend on load conditions, which would influence the overall performance, several SYS-ID procedures were performed under various conditions (indoor: helicopter on skid, rubber wheels, freely suspended; outdoor: ground idle, flight idle, LF). Based on this data the robustness and the performance was estimated in theoretical simulations and validated during flight [3] [4] [5].

3. FLIGHT TEST RESULTS

In order to demonstrate the performance of the active system at the most common flight regimes level flights at different air speed, RPM sweeps, curve flights, hover and flares have been performed. Main emphasis was to demonstrate jet smooth helicopter ride independent from operational conditions and rotor speed variations [6].

The AVC prototype system was designed based on EC135 and EC145 requirements. All flight tests were performed on non-serial helicopters.

Figure 5: Exemplary rotorcraft types used for AVC

Different stages of system and control complexity, depending on platform specific requirements with respect to actuation direction, frequency and force have been investigated.

- 1-axis control in lateral (y) direction
- 1-axis control in vertical (z) direction
- 2-axis control in both (y / z) directions

The most interesting results out of these experiments are presented hereafter. Because the AVC system was tested on several light/medium helicopters all figures have been normalized to the maximum N/rev vibration value of the corresponding reference case. The qualitative reduction values are therefore with respect to this normalized maximum.

3.1. Lateral Active Vibration Control (1-axis)

The lateral AVC system consisted of two force generators located in y-direction in the pilot/copilot plane. Multiple accelerometers were located in this plane and in addition at the passenger seat plane as well as the rear compartment plane. Figure 6 and 7 show the flight test results for rpm sweep at Vh.

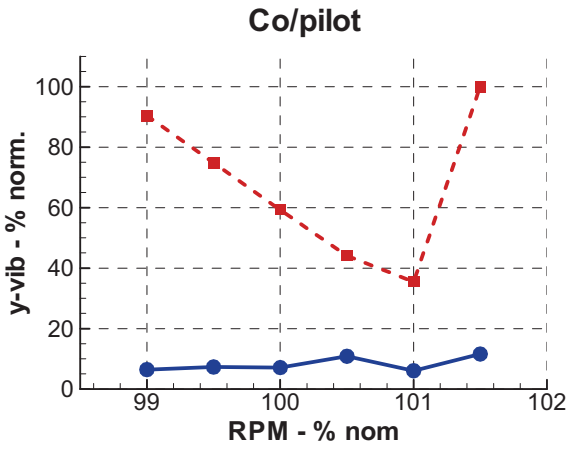

Figure 6: Lateral N/rev vibration level reduction at pilot/copilot seat plane at RPM sweep

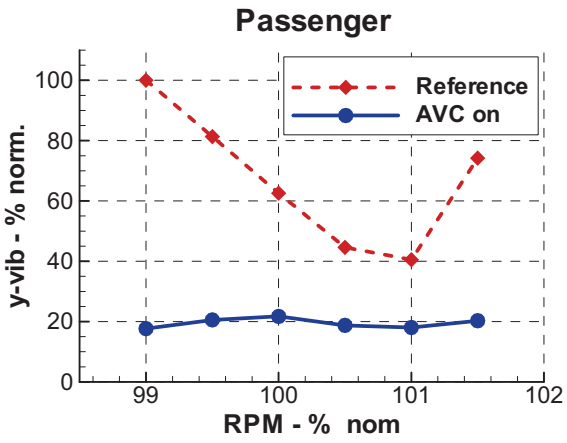

Figure 7: Lateral N/rev vibration level reduction at passenger seat plane at RPM sweep

The figures demonstrate that the AVC system ensures considerable vibration level reduction, in-between 20% to 90%, over the entire rpm range. Additionally, the vibrations are consistently below the reference helicopter with a well-tuned passive lateral absorber, which is limited to a small bandwidth - here in-between 100.5 and 101% nom. RPM. Another disadvantage of the passive reference system is that its efficiency is maximum at the clamping position (local nodal point) instead of for instance the copilot position as used by the AVC system.

Following, the improvement holds when lateral vibrations are plotted over flight speed as displayed in figure 8 and 9. In particular, in the pilot/copilot plane the substantial reduction with respect to the reference is clearly visible (60% to 80%). The apparently reduced improvement in figure 9 (40% to 60%) is explained by the control scenario used in this specific flight case taking only sensors at the co/pilot plane into account.

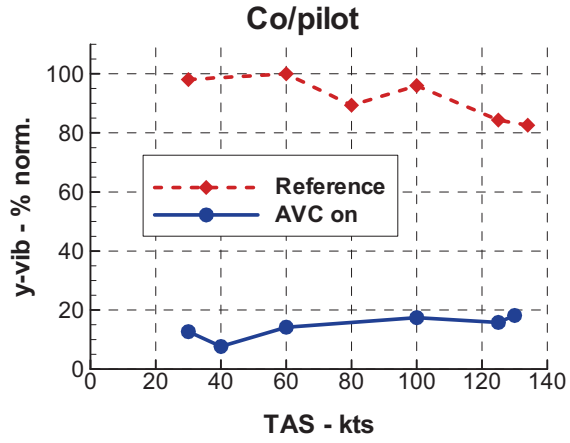

Figure 8: Lateral N/rev vibration level reduction at pilot/copilot seat plane at level flight

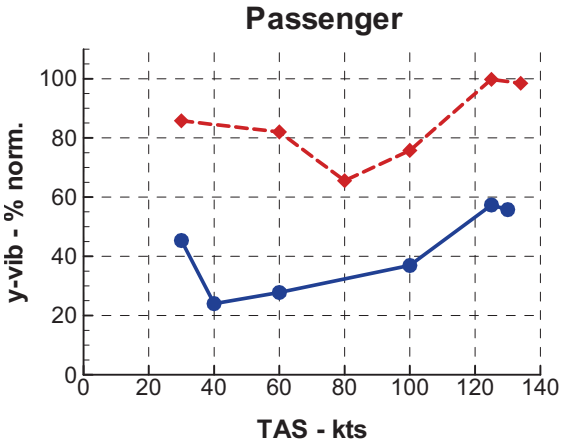

Figure 9: Lateral N/rev vibration level reduction at passenger seat plane at level flight

3.2. Vertical Active Vibration Control (1-axis)

In case of vertical AVC, the system consisted of four force generators equally divided at the pilot/copilot and passenger area. Six accelerometers were used for control purpose and eight sensor locations on the cabin floor were used for monitoring. Figure 10 presents a spatial overview of the vibration reduction in level flight at all sensor positions with respect to the reference case. The right-hand plot represents the reference with passive absorbers and the left-hand picture is with AVC on.

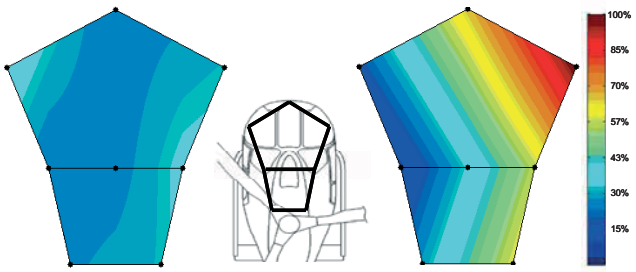

Figure 10: Vibration level reduction at cabin floor at level flight with 130kt IAS.

The first effect of the AVC system on the vibrations magnitude is a tremendous local reduction at the right hand side of the helicopter. Considerable effort of the controller was performed to relocate and optimize force and phase from the local nodal point to the control sensor position. The second effect is that the AVC generally changed the dynamics and showed a well-balanced cabin floor in terms of vibrations.

3.3. 2-Axis Active Vibration Control

The highest degree of system complexity proven during flight tests was a 2-axis controller. In this case 2 lateral and 2 vertical force generators were installed in the helicopter. The ultimate goal of the

flight test was to reduce the human perceived vibrations at the location of control independent of flight condition. To take the directional dependant perception into account, an intrusion index was used to adjust the vertical and lateral vibration level to the same "feeling" level. A scaling factor was implemented in the controller based on nominal rotor speed, because humans are more sensitive to vibrations in vertical direction as in lateral direction. Three specific flight conditions are examined hereafter: RPM variation, turn and flares.

3.3.1. RPM sweep

As mentioned before, the ability to cope with RPM variation is of major importance for future helicopters. In line with the results already demonstrated for the 1-axis system, Figure 11 and 12 present vibration reduction of the 2-axis system in vertical and lateral direction, respectively. Equally good performance of the AVC system is identified, with again cabin vibration reduction values up to 90% in z direction and in-between 50-90% in y-direction.

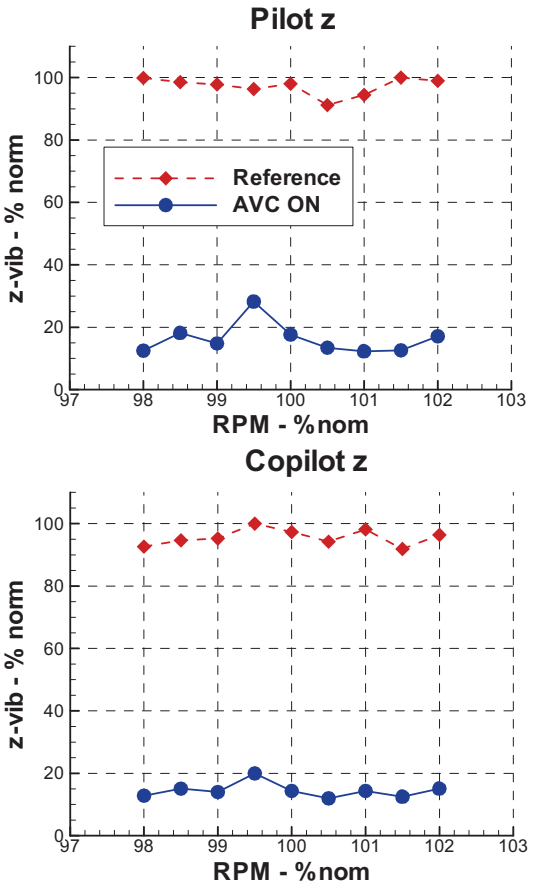

Figure 11: Vibration level reduction (N/rev) for RPM variation at Vh in z-direction.

Evidently the increase of complexity did not relate to efficiency decrease of the AVC system and proved its robustness. Also observable from the figures is that, in contrary to the 1-axis system, the performance of the reference platform is not strongly

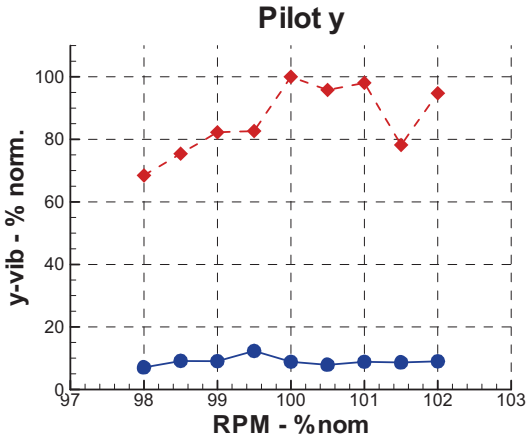

Figure 12: Vibration level reduction (N/rev) for RPM variation at Vh in y-direction.

RPM frequency dependent. This is due to semi-active absorbers (frequency adaptive) installed in the reference helicopter.

3.3.2. Turns

To demonstrate the capability of the AVC system at higher load factors, curve flights have been performed at 100kt. Depending on different bank angle (15°, 30°) loads up to ~1.8g could be obtained.

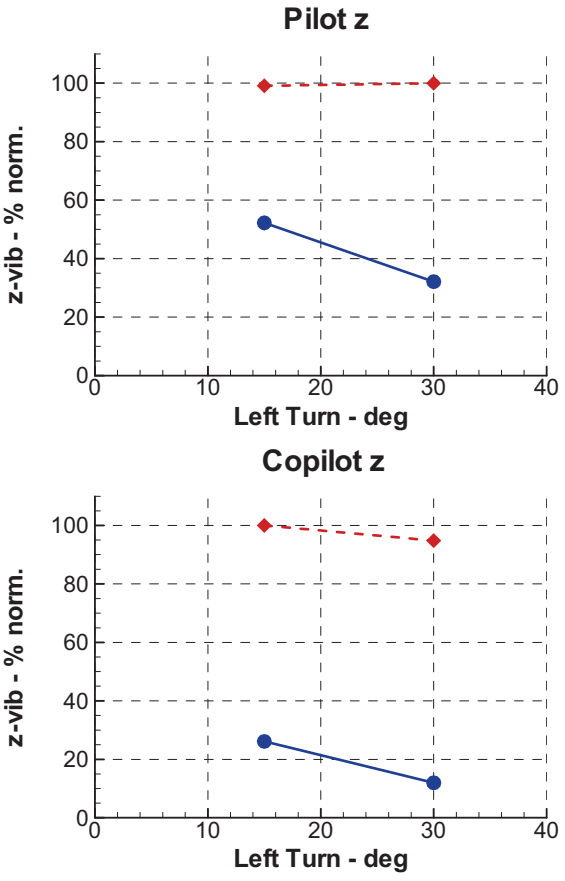

Figure 13: Vibration level reduction (N/rev) at high load factor flights with different bank angle.

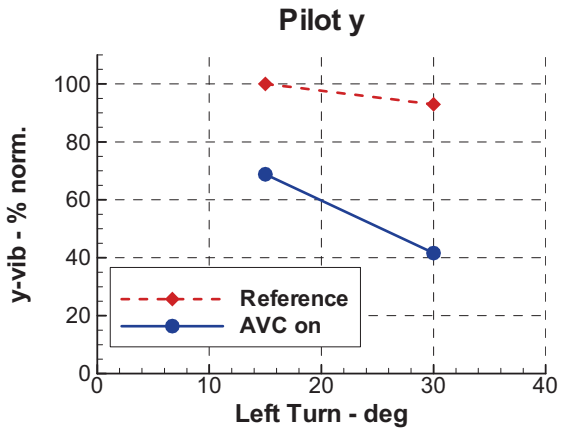

Figure 14: Vibration level reduction (N/rev) at high load factor flights with different bank angle.

Figure 13 and 14 show the percentage reduction at the control positions in relation with the reference with semi-active absorbers. As shown in this figure the AVC system works properly and vibration reduction in-between 35-80% could be achieved. The controller behaved stable irrespective of the high load on the structure and the active system.

3.3.3. Flares

Figure 15 summarizes the percentage vibration reduction against time with and without AVC at the control positions. Two kinds of flares are presented: long and short. The flare manoeuvre goes mostly along with high vibration levels varying on its length and the helicopter speed. Such unsteady flight regimes are challenging for active systems to no little extent due to severe vibration levels and their near to transient nature. For these reasons tests have been performed to optimize the controller convergence properties and to find the stability limits for this special flight regime. In particular for the short flare manoeuvre high tracking capability of the controller is required, which can be adjusted by the step size α. On the other hand very high open loop amplification and controller bandwidth increases the risk of controller instability in case the plant is not perfectly known e.g. due to nonlinearities in the system. This conflict of objectives explains the differences on performance of the AVCS between long and short flares (see Figure 15 Pilot y).

However, the AVC system performed always stable during all flares and significant vibration level reduction, in-between 35-60% for the short flare and in-between 70-90% for the long flare could be achieved in vertical direction, which is the more significant for human perception.

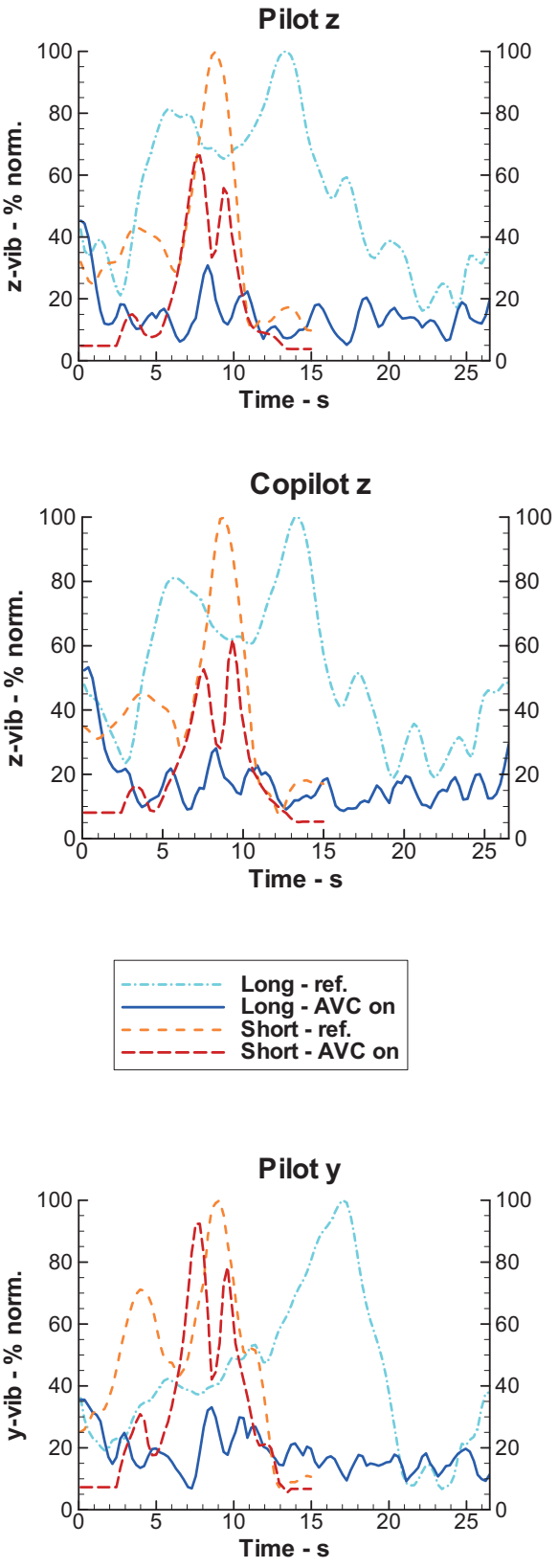

Figure 15: Vibration level reduction (N/rev) during normal and long flare.

4. CONCLUSIONS

In future, the greening of air transport will demand wider rotor rpm ranges in order to optimize for both low external noise levels and high fuel efficiency. In order to adapt to these rpm variations, the spread of active systems will further increase and substitute more and more passive systems with fixed frequency tuning.

Recent advances in Eurocopter's activities on the cabin active vibration control (AVC) system have been presented in this paper. An overview of the complete system design is given as well as an evaluation of the most important results achieved during several flight tests on different light and medium rotorcrafts.

During all flight tests on different sized platforms the AVC system showed superior performance, due to its capability of frequency and amplitude adaptation.

In general, the AVC system yields in very low vibration levels, compared to current passive or semi-active absorbers, in several level flight conditions including RPM changes, turns and flares. This proves that AVC exhibits the genuine ability to manage cabin vibrations in the demanding future.

Summarized, the AVC system is a highly efficient, weight optimized and cost competitive system that is able to reduce significantly the rotor-induced vibration levels and ensures Eurocopter target to achieve the long-envisaged jet-smooth ride comfort.

5. ACKNOWLEDGMENTS

The present work was performed in close collaboration with EADS Innovation Works.

6. REFERENCES

[1] Braun, D., "*Development of Antiresonance Force Isolators for Helicopter Vibration Reduction*", 6th European Rotorcraft and Powered Lift Forum, September 1980.

[2] Konstanzer P., Jänker P., Storm S., *A piezo inertial force generator optimized for high force and low frequency*, Smart Materials and Structures 16, 1260-1264, 2007

[3] Hoffmann F., Maier R., Jänker P., Hermle F., Berthe A., *Helicopter Interior Noise Reduction by using Active Gearbox Struts*, 12th AIAA/CEAS Aeroacoustic Conference, AIAA-2006-2604, Cambridge, MA, 8-10 May 2006

[4] Maier R., Hoffmann F., Tewes S., Bebesel M., *Active Vibration Isolation System for Helicopter Interior Noise Reduction*, 8th AIAA/CEAS Aeroacoustic Conference, AIAA 2002-2495, Breckenridge, Colorado, 2002

[5] Elliot S. J., Nellson P. A., *Active Control of Sound*, Academic Press, Harcourt Brace Jovanovich, 1992

[6] Konstanzer P., Enenkl B., Aubourg P.A., Cranga P., *Recent advances in Eurocopter's passive and active vibration control*, AHS Conference, Montreal, Canada, 2008